Astronomy & Astrophysics manuscript no. 3010 February 5, 2008
(DOI: will be inserted by hand later)

XMM-Newton X-ray and optical observations of the globular clusters M 55 and NGC 3201

N.A. Webb[1], P.J. Wheatley[2], and D. Barret[1]

[1] Centre d'Etude Spatiale des Rayonnements, 9 avenue du Colonel Roche, 31028 Toulouse Cedex 04, France
[2] Department of Physics and Astronomy, University of Leicester, Leicester LE1 7RH, England

Received 2005; accepted 2005

Abstract. We have observed two low concentration Galactic globular clusters with the X-ray observatory *XMM-Newton*. We detect 47 faint X-ray sources in the direction of M 55 and 62 in the field of view of NGC 3201. Using the statistical Log N-Log S relationship of extragalactic sources derived from *XMM-Newton* Lockman Hole observations, to estimate the background source population, we estimate that very few of the sources (1.5±1.0) in the field of view of M 55 actually belong to the cluster. These sources are located in the centre of the cluster as we expect if the cluster has undergone mass segregation. NGC 3201 has approximately 15 related sources, which are centrally located but are not constrained to lie within the half mass radius. The sources belonging to this cluster can lie up to 5 core radii from the centre of the cluster which could imply that this cluster has been perturbed. Using X-ray (and optical, in the case of M 55) colours, spectral and timing analysis (where possible) and comparing these observations to previous X-ray observations, we find evidence for sources in each cluster that could be cataclysmic variables, active binaries, millisecond pulsars and possible evidence for a quiescent low mass X-ray binary with a neutron star primary, even though we do not expect any such objects in either of the clusters, due to their low central concentrations. The majority of the other sources are background sources, such as AGN. ⋆

Key words. globular clusters: individual:M 55 - NGC 3201 – X-rays: general – binaries: general – stars: variables: general

1. Introduction

Following the discovery, over twenty years ago, of low luminosity ($L_x \lesssim 10^{34.5}$ erg s^{-1}) X-ray sources in globular clusters (Hertz & Grindlay, 1983), the known population of such sources has steadily grown (e.g. Johnston & Verbunt, 1994; Cool et al., 1995; Johnston et al., 1996; Geffert et al., 1997; Verbunt, 2001). However, with the launch of the X-ray observatories *XMM-Newton* and *Chandra*, whose sensitivity and angular resolution (respectively) far surpasses those of previous X-ray observatories, the number of new sources detected (and identified) has truly flourished (e.g. Webb et al., 2004c; Gendre et al., 2003a; Pooley et al., 2003; Heinke et al., 2003; Gendre et al., 2003b; Rutledge et al., 2002; Webb et al., 2001; Grindlay et al., 2001). The low luminosity X-ray sources that belong to their respective clusters are mostly a variety of binary systems (X-ray binaries, cataclysmic variables and active binaries) as well as descendants of these objects (such as millisecond pulsars). These X-ray sources are thus indispensable objects with which to complete the study of stellar and globular cluster evolution, stellar dynamics, binary formation and evolution, as well as the study of the binaries themselves, see e.g. Verbunt & Lewin (2004); Hut et al. (1992) for reviews of these topics.

Send offprint requests to: N.A. Webb e-mail: Natalie.Webb@cesr.fr

We have thus observed two further globular clusters (M 55 (NGC 6809) and NGC 3201) using *XMM-Newton*, to detect their populations of low luminosity X-ray sources and determine the nature of these sources, as well as probe the evolution of the clusters.

The two globular clusters presented in this paper are particularly interesting to study as they have very low central concentrations of stars. It is thought that through dynamical evolution, cluster cores become increasingly concentrated (Hénon, 1961). Stellar encounters in globular clusters result in an equipartition of energy. Through virialization, the more massive stars of the cluster, such as degenerate objects and binary systems, are concentrated towards the centre of the cluster. Low concentration clusters are therefore least affected by dynamical processes and thus mass segregation is thought to be less important for these clusters than the higher concentration clusters. These clusters are also particularly susceptible to tidal shocking (Chernoff et al., 1986) and to a loss of stars from the cluster.

Both clusters have been studied at long and short wavelengths. M 55 has previously been observed in the X-ray domain by the X-ray telescopes *Ariel V* (Pye & McHardy, 1983), *EINSTEIN*, *HEAO 1* (Hertz & Wood, 1985) and *Rosat* (Johnston et al., 1996; Verbunt, 2001). Pye & McHardy (1983) found a transient source with *Ariel V*, that lies towards the edge of the cluster (outside the field of view of our observations). Johnston et al. (1996) found 18 sources with the *Rosat*

PSPC. A number of studies in the optical domain have analysed the nature of the cluster through the study of its luminosity function and the distribution of stars, blue stragglers, binary systems and variable stars e.g. Piotto & Zoccali (1999); Zaggia et al. (1997); Mandushez et al. (1997); Pych et al. (2001); Olech et al. (1999).

NGC 3201 has also been studied with the X-ray telescopes *HEAO 1* (Hertz & Wood, 1985) and *Rosat* (Johnston et al., 1996; Verbunt, 2001). Nine sources were found by Johnston et al. (1996) and an additional one by Verbunt (2001). This cluster has also been extensively studied in the optical domain e.g. Layden & Sarajedini (2003); Mazur et al. (2003); Covey et al. (2003); Piersimoni et al. (2002); von Braun & Mateo (2002).

2. Observations and data reduction

2.1. X-ray data

We obtained *XMM-Newton* observations of the two globular clusters M 55 and NGC 3201, during the 'Routine Observing Phase'. The observations are given in Table 1. Approximately 3 and 4 ks of the *pn* data of the two clusters respectively were affected by high background activity (a soft proton flare). All of the data were reduced with version 6.0 of the *XMM-Newton* SAS (Science Analysis Software).

The MOS data were reduced using the 'emchain' with 'embadpixfind' to detect the bad pixels. The event lists were filtered, so that 0-12 of the predefined patterns (single, double, triple, and quadruple pixel events) were retained and the high background periods were identified by defining a count rate threshold above the low background rate and the periods of higher background counts were then flagged in the event list. We also filtered in energy. We used the energy range 0.2-10.0 keV, as recommended in the document 'EPIC Status of Calibration and Data Analysis' (Kirsch et al., 2002).

The *pn* data were reduced using the 'epchain' of the SAS. Again the event lists were filtered, so that 0-4 of the predefined patterns (single and double events) were retained, as these have the best energy calibration. We again filtered in energy, where we used the energy range 0.5-10.0 keV.

Table 1. Summary of the observations presented in this paper

Cluster/ Date	Instrument	Filter	Mode	Useful exposure (ks)
M 55/	MOS	medium	Full frame*	26
17-18/10/01	pn	medium	Full frame	24
	OM	UVW2, B	Imaging	2×1, 1
NGC 3201/	MOS	medium	Full frame	40
25/05/03	pn	medium	Full frame	42
	OM	UVW1	Imaging	2×4.82, 0.8

* Turner et al. (2001)

The source detection was done in the same way as Gendre et al. (2003a); Webb et al. (2004c), but in summary we used the SAS wavelet detection algorithm on the 0.5-5.0 keV image, as the signal-to-noise ratio was best in this range. We kept only those sources detected with two or more cameras,

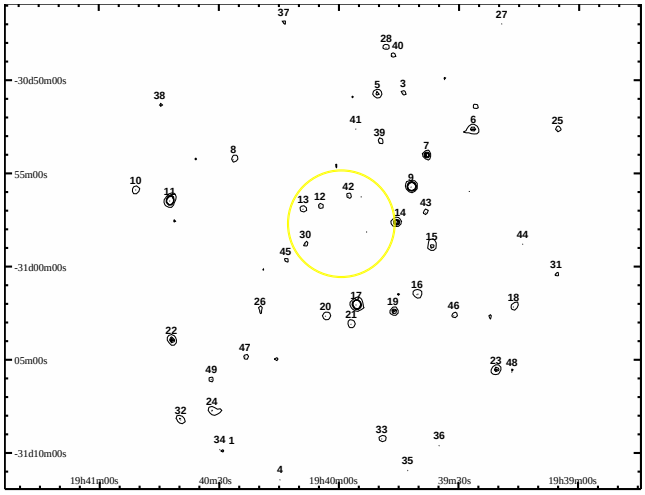

Fig. 1. X-ray contour plot of the central region of M 55. The circle shows both the core and the half-mass radii which are almost coincident. The abscissa indicates the right ascension in ^{h} ^{m} ^{s} and the ordinate indicates the declination in $^\circ$ $'$ $''$. The contours represent 4, 6 and 8 σ confidence levels and the source numbers are those found in Table 2.

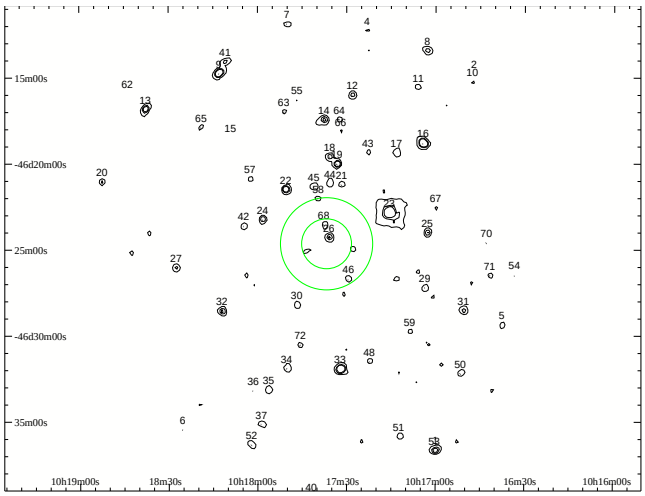

Fig. 2. X-ray contour plot of the central region of NGC 3201 (similar to Fig. 1). The source numbers are those found in Table 3. Source 23 looks slightly extended in this combined image, but it is a point source.

with the exception of sources found with the *pn* camera, which is more sensitive than the two MOS cameras. We detected 47 sources in the field of view (FOV) (radius~15′) of M 55 and 62 sources in the FOV of NGC 3201, with a maximum likelihood greater than 4.5σ. These sources are given in Tables 2 and 3, along with their position and count rate. We also give the identification number for the sources detected by *Rosat*. The positional error is the 90% confidence mean statistical error on the position of the *XMM-Newton* sources. The majority of these sources can be seen in the contour plots of the central regions of these globular clusters, see Figs. 1 and 2.

Table 2. X-ray sources in the direction of M 55, as determined from the EPIC observations, 0.5-10.0 keV band. The identification number, any former identifications and position are given, along with the error on this position and the count rate.

ID	For. ID	RA (2000) h m s	Dec (2000) ° ′ ″	Error ″	Count s^{-1} $\times 10^{-3}$
1		19 40 29.04	-31 9 54.36	7.96	3.96±0.95
3		19 39 44.00	-30 50 42.98	6.74	3.85±0.76
4		19 40 14.76	-31 11 27.67	6.78	8.09±1.30
5		19 39 50.40	-30 50 47.18	4.98	10.87±1.21
6		19 39 26.38	-30 52 40.32	4.88	16.69±1.52
7		19 39 38.14	-30 54 4.60	4.52	10.92±0.91
8		19 40 26.43	-30 54 16.95	6.23	4.84±0.73
9	6	19 39 41.92	-30 55 45.88	4.20	26.30±1.34
10	7	19 40 50.85	-30 55 54.31	5.22	13.72±1.69
11	8	19 40 42.35	-30 56 30.12	4.22	50.59±2.55
12[c]		19 40 4.75	-30 56 46.84	9.60	1.27±0.31
13[c]		19 40 8.96	-30 56 57.26	5.91	3.34±0.59
14[h]		19 39 45.77	-30 57 40.14	4.46	10.44±0.98
15		19 39 36.78	-30 58 56.86	4.80	8.24±0.80
16		19 39 40.44	-31 1 31.48	4.96	7.43±0.85
17	13	19 39 55.69	-31 2 5.01	4.17	31.60±1.49
18		19 39 16.28	-31 2 11.08	5.08	7.28±0.97
19		19 39 46.46	-31 2 26.91	4.60	8.40±0.84
20		19 40 3.36	-31 2 41.65	5.13	6.29±0.82
21		19 39 56.94	-31 3 7.61	4.87	5.83±0.72
22	15	19 40 41.98	-31 3 58.28	4.54	21.08±1.84
23		19 39 20.68	-31 5 33.77	4.78	15.68±1.57
24		19 40 31.87	-31 7 45.96	5.01	17.20±1.90
25	5	19 39 5.34	-30 52 41.18	5.97	7.94±1.32
26		19 40 19.76	-31 2 25.13	11.44	1.43±0.37
27		19 39 19.35	-30 46 59.67	7.58	3.76±0.89
28		19 39 48.21	-30 48 17.35	5.70	6.29±1.14
30[c]	9	19 40 8.40	-30 58 48.82	6.98	1.40±0.30
31	12	19 39 5.63	-31 0 25.46	6.94	2.34±0.53
32		19 40 39.67	-31 8 15.00	4.82	20.02±2.26
33		19 39 49.26	-31 9 16.30	5.70	8.56±1.25
34		19 40 29.88	-31 9 50.29	7.21	4.00±0.87
35		19 39 42.75	-31 10 57.82	7.45	2.17±0.59
36		19 39 34.83	-31 9 37.49	10.97	3.24±0.89
37		19 40 13.80	-30 46 56.34	7.83	4.37±1.02
38		19 40 44.85	-30 51 21.35	9.39	5.07±1.41
39		19 39 49.82	-30 53 21.63	8.04	1.98±0.52
40		19 39 46.74	-30 48 42.22	7.96	3.94±0.91
41		19 39 55.79	-30 52 39.14	7.26	1.74±0.43
42[c]		19 39 57.64	-30 56 13.82	8.52	2.11±0.47
43		19 39 38.26	-30 57 8.22	7.52	2.15±0.49
44		19 39 14.01	-30 58 49.21	7.98	2.00±0.60
45		19 40 13.380	-30 59 43.71	7.33	1.60±0.43
46		19 39 31.25	-31 2 39.44	6.25	2.28±0.52
47		19 40 23.55	-31 4 52.85	7.98	3.07±0.81
48		19 39 16.66	-31 5 41.05	6.88	3.34±0.79
49	16	19 40 31.96	-31 6 4.79	8.00	4.23±1.02

[c] sources within the core, [h] sources within the half mass radius numbers, *Rosat* PSPC, Johnston et al. (1996)

2.2. Optical data

The *XMM-Newton* optical monitor (Mason et al., 2001) was also employed during the X-ray observations and the data obtained is given in Table 1. The data were reduced using the standard SAS *omichain* script.

We find 345 stars with a minimum significance of 3.0 in the FOV of M 55, detected in both the UVW2- and the B-band. The magnitudes range from approximately 14.0 to 19.5 in the UVW2-filter and 12.0 to 20.5 in the B-filter. The photometric errors are poor for the UVW2-filter ranging from 0.001 to 1.5 magnitudes with a mean value of 0.22, but better for the B-filter, ranging from 0.001-0.6 magnitudes with a mean value of 0.03.

We find 7569 stars with a minimum significance of 3.0 in the FOV of NGC 3201. The magnitudes range from approximately 12 to 22 with photometric errors ranging from 0.001 to 1.5 magnitudes with a mean value of 0.17. However, as the observations have been made using a single filter (UVW1), these data are of limited use in determining the optical counterparts to the X-ray sources.

3. The X-ray sources

3.1. M 55

We have detected four sources within the core radius (2.83′, centred at RA=19^h 39^m 59.40^s, dec=-30° 57′ 43.5″ Djorgovski, 1993) of M 55, sources 12, 13, 30, and 42 (indicated by a [c] in Table 2), and a further source (14) that lies just on the limit of the half-mass radius (2.89′ Harris, 1999) (indicated by a [h] in Table 2). We computed the detectable flux limit within the half mass radius, assuming a 0.6 keV blackbody spectral model in the same way as Johnston & Verbunt (1996). The limiting luminosity at the centre of the field of view for the *pn* camera is $L_x = 7 \times 10^{30}$ erg s^{-1} (0.5-10.0 keV) and $L_x = 2 \times 10^{31}$ erg s^{-1} (0.5-10.0 keV) for the MOS.

Many of our detected sources are background sources. We have used the statistical Log N-Log S relationship of extragalactic sources derived from the Lockman Hole observations (Hasinger et al., 2001) to estimate the background source population, assuming that there is no cosmic variance. We converted the source count rates to fluxes using a power law model with a spectral index of -2, as Hasinger et al. (2001). We employed the method of Cool et al. (2002) and Gendre et al. (2003a) which takes into account vignetting, as the faintest detectable flux increases with radius. We calculated the average limiting flux in three annuli on the *pn* camera, in the same way as Johnston & Verbunt (1996). These annuli were bound by the core/half-mass radii, three and five core radii. We expect 3.5±1, 21.2±2 and 22.3±5 background sources in these annuli respectively. The uncertainty is the 10% error estimated on the flux, as Hasinger et al. (2001). We find 5, 17 and 25 sources in these annuli respectively. Although the sample is small and therefore the results are not very robust, this indicates that at least one of the core/half-mass radii sources is likely to belong to the cluster. Using the 5 sources found in the half mass radius and the fact that approximately 1.5 may belong to the cluster, we calculate using Poisson statistics, that the probability that none of the 5 sources are cluster members is 27%. This supports the idea that not all the core sources belong to the cluster.

It is also possible to calculate the probability that the sources within the core are not simply spurious identifications with the cluster, in the same manner as Verbunt (2001). The probability (p) that one serendipitous source in the *pn* observation is at a distance $r < R$ to the cluster centre, where R is the core radius, is $p = (R/r_d)^2$, where r_d is the radius of the field of view. The probability of a randomly located source falling within the core radius is 3.6 percent. For the 47 sources, the probability of finding no sources within the core radius by chance is (1-p)×47 = 18%. This again supports the assertion that not all the core sources belong to the cluster.

3.2. NGC 3201

NGC 3201, centred at RA=10^h 17^m 36.8^s, dec=-46° 24′ 40″ (Harris, 1999), has fewer centrally located X-ray sources. Within the core radius (1.45′ Djorgovski, 1993), we find only two sources, sources 26 and 68 (indicated by a [c] in Table 3). We find another two in the half-mass radius (2.68′ Harris, 1999), sources 46 and 58 (indicated by a [h] in Table 2). The limiting luminosity for the *pn* camera is $L_x = 8 \times 10^{30}$ erg s^{-1} (0.5-10.0 keV) and $L_x = 2 \times 10^{31}$ erg s^{-1} (0.5-10.0 keV) for the MOS camera.

To determine the number of expected background sources, we defined six annuli bound by the core radius, the half-mass radius, 3, 5, 7.5 and 10 core radii. We expect 0.7±0.1, 1.8±0.4 and 3.3±0.7, 7.3±2.0, 13.8±2.0 and 18.4±2.0 background sources in these annuli. We find 2, 2, 7, 17, 15 and 19 sources in these annuli respectively. This indicates an overdensity of sources in almost every annulus, except the outer two, which is different to many other globular clusters and is discussed in Section 5. Using the 4 sources found in the half mass radius and the fact that approximately 1.5 may belong to the cluster, we calculate using Poisson statistics, that the probability that none of the 4 sources are cluster members is 24%. This supports the idea that not all the core sources belong to the cluster. The probability of a randomly located source not falling in the core radius is 99.0%. For the 62 sources, the probability of finding no sources within the core radius by chance is 55%. It is therefore likely that at least one of the core sources does belong to the cluster.

However, as stated above, we find an excess of sources in many of the defined annuli. Considering the four innermost annuli, we find 28 sources where we expect approximately 13. Poisson statistics indicate that the probability that none of these sources belong to the cluster is 0.02%. This implies that at least one of the sources does belong to the cluster.

3.3. Spectral analysis

Seven X-ray sources in M 55 and nine sources in NGC 3201 have enough counts that we could extract and fit the spectra. We extracted the spectra using circles of radii ∼1′ centred on the source, with the exception of source 19 in NGC 3201 where we used an extraction radius of ∼30″ due its close proximity to other sources. We used a similar neighbouring region, free from X-ray sources to extract a background file. We re-

Table 3. As Table 2 but in the direction of NGC 3201.

ID	For. ID	RA (2000) h m s	Dec (2000) ° ′ ″	Error ″	Count s^{-1} ×10^{-3}
1		10 16 59.90	-46 36 38.90	4.94	14.12±1.27
2		10 16 47.23	-46 14 49.24	7.67	1.48±0.37
4		10 17 23.13	-46 12 18.22	5.49	6.12±1.19
5		10 16 37.66	-46 29 24.73	5.58	6.50±0.99
6		10 18 25.40	-46 35 28.63	6.17	4.39±1.04
7		10 17 50.21	-46 11 55.97	6.36	8.72±1.27
8		10 17 2.89	-46 13 29.03	4.84	16.62±1.55
9	3	10 18 13.00	-46 14 47.19	4.24	49.28±2.49
10		10 16 47.76	-46 15 16.54	7.34	1.85±0.49
11		10 17 5.97	-46 15 36.15	5.02	7.07±1.17
12		10 17 28.11	-46 16 3.52	4.97	10.00±1.04
13	4	10 18 37.76	-46 16 52.53	4.33	39.19±2.62
14		10 17 37.70	-46 17 29.72	4.51	13.27±1.01
15		10 18 9.13	-46 18 32.61	8.37	1.83±0.46
16		10 17 4.28	-46 18 50.88	4.17	35.43±1.61
17		10 17 13.26	-46 19 25.62	5.02	6.13±0.70
18		10 17 35.76	-46 19 39.84	4.70	6.94±0.72
19		10 17 33.26	-46 20 3.51	4.28	13.74±0.88
20		10 18 52.44	-46 21 5.50	4.86	22.21±2.06
21		10 17 31.72	-46 21 15.74	5.95	2.53±0.41
22		10 17 50.54	-46 21 32.90	4.25	15.75±0.96
23	6	10 17 15.63	-46 22 54.06	4.04	87.13±1.55
24		10 17 58.33	-46 23 17.00	4.55	8.07±0.71
25		10 17 2.85	-46 24 3.93	4.65	8.07±0.71
26[c]	C	10 17 36.00	-46 24 19.50	4.57	7.09±0.58
27		10 18 27.54	-46 26 3.48	4.97	10.18±1.08
29		10 17 3.64	-46 27 15.52	5.37	3.44±0.53
30		10 17 46.85	-46 28 15.00	4.99	4.13±0.53
31		10 16 50.58	-46 28 35.89	4.81	9.21±0.88
32		10 18 12.08	-46 28 36.49	4.60	12.63±1.0
33		10 17 32.20	-46 31 57.59	4.27	24.90±1.35
34		10 17 50.25	-46 31 57.61	5.19	5.96±0.80
35		10 17 56.34	-46 33 11.57	5.01	7.34±0.89
36		10 18 1.57	-46 33 15.41	6.68	3.81±0.75
37		10 17 58.81	-46 35 11.47	5.11	8.80±1.12
40		10 17 41.92	-46 39 22.59	10.11	2.45±0.62
41		10 18 10.89	-46 14 6.96	5.00	12.81±1.39
42		10 18 4.76	-46 23 40.79	5.57	4.40±0.61
43		10 17 22.86	-46 19 23.53	6.36	2.34±0.45
44		10 17 35.68	-46 21 11.29	5.27	4.08±0.55
45		10 17 41.08	-46 21 22.55	5.18	3.96±0.56
46[h]		10 17 29.42	-46 26 44.96	5.49	2.98±0.45
48		10 17 22.36	-46 31 34.01	5.49	3.29±0.51
50		10 16 51.55	-46 32 13.14	5.75	5.79±0.85
51		10 17 12.40	-46 35 54.46	5.40	6.54±0.98
52		10 18 2.11	-46 36 22.69	5.39	10.80±1.41
53		10 17 0.35	-46 36 42.83	4.96	10.63±1.09
54		10 16 33.37	-46 26 30.55	8.78	3.26±0.76
55		10 17 46.74	-46 16 20.56	8.53	2.44±0.62
57		10 18 2.61	-46 20 54.86	8.38	1.99±0.46
58[h]		10 17 39.60	-46 22 3.71	8.03	1.46±0.35
59		10 17 8.71	-46 29 47.34	8.67	1.72±0.45
62		10 18 43.83	-46 15 57.42	5.21	13.16±1.74
63		10 17 51.18	-46 17 3.33	6.95	2.59±0.59
64		10 17 32.48	-46 17 29.54	8.04	1.74±0.51
65		10 18 19.01	-46 17 55.49	6.71	3.88±0.82
66		10 17 32.07	-46 18 10.60	7.40	1.45±0.40
67		10 17 0.38	-46 22 36.30	7.31	2.09±0.50
68[c]		10 17 37.72	-46 23 36.30	9.90	1.43±0.37
70		10 16 42.89	-46 24 37.22	7.36	2.09±0.6
71		10 16 41.75	-46 26 32.46	6.89	2.85±0.63
72		10 17 45.66	-46 30 35.88	7.24	1.76±0.45

binned the MOS data into 15 eV bins and the *pn* data into 5eV bins. We used the SAS tasks 'rmfgen' and 'arfgen' to generate a 'redistribution matrix file' and an 'ancillary response file', for each source. We binned up the data to contain at least 20 net counts/bin. We then used Xspec (Version 11.2.0) to fit the spectra. We initially tried simple models, such as a power law, a blackbody, a bremsstrahlung and a Raymond Smith fit, allowing the absorption and the model parameters to vary freely, so that the best fit values obtained do not depend on the initial parameters chosen for the model. If the fit could not be constrained with the freely varying absorption value, we fixed the absorption value to that of the cluster. We found that simple models provided a good fit to the data for the majority of the sources. However, we found that for certain sources, we required a more complicated model to fit the data. The results of the spectral fitting can be found in Tables 4 and 5, where the best fits are given, along with the goodness of fit (χ^2_ν) and the flux in the 0.2-10.0 keV range.

As the rest of the sources have insufficient counts to extract a spectrum, we have used colour-colour diagrams (see Figs. 3 and 4) to derive information about their spectral form.

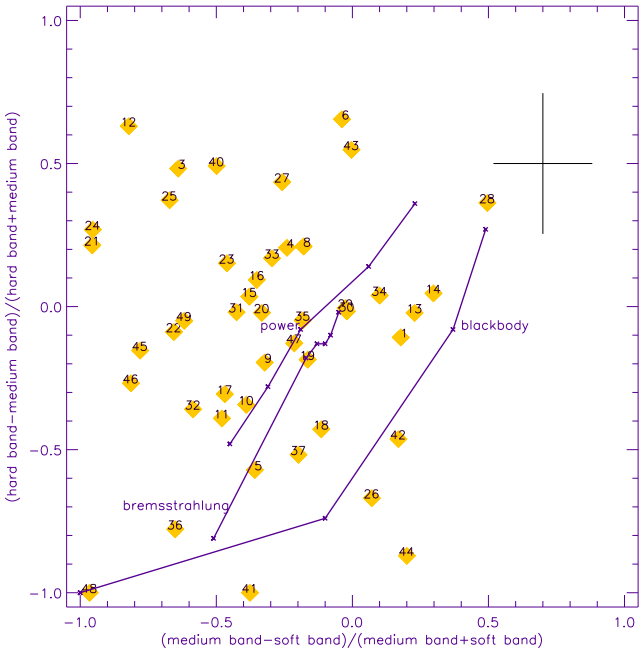

Fig. 3. An X-ray colour diagram of the detected X-ray sources in M 55. Diamonds with a number indicate an X-ray source where the number is that given in Table 2. The hard band is 3.0-10.0 keV, the medium band is 1.5-3.0 keV and the soft band is 0.5-1.5 keV. Three lines are indicated showing the colours of a hypothetical source in the cluster with a power law spectrum, a bremsstrahlung spectrum and a blackbody spectrum. On the power law spectrum line, the crosses (from bottom to top) represent photon indices of 2.5, 2.0, 1.5, 1.0 and 0.5. On the bremsstrahlung spectrum line, the crosses (from bottom to top) represent temperatures of 1.0, 5.0, 10.0, 15.0 and 30.0 keV. On the blackbody spectrum line, the crosses (from bottom to top) represent temperatures of 0.1, 0.5, 1.0, 1.5 keV. For N_H values greater than that of the cluster, the spectral fits move towards the top right. A typical error bar is also shown in the top right hand corner.

3.4. Variability analysis

We carried out variability tests on all the sources by dividing the data into two equal frames (10 ks for M 55 and 20 ks for NGC 3201) and then into four equal frames (5 ks for M 55 and 10 ks for NGC 3201). We looked for variability, defined by a change in the frame to frame count rate by more than the statistical error for each frame (calculated by the source detection chain). Using this method we found variable sources in both clusters. Sources 22 and 37 in M 55 are variable. Using the χ^2 probability of constancy test, these two sources are variable at the 1 and 3 σ level respectively. In NGC 3201, sources 42, 45, 55 and 63 are variable. Again using the χ^2 probability of constancy test, these sources are variable at the 4, 2, 2 and 2 σ levels respectively.

We also carried out a different variability analysis on the sources given in Tables 4 and 5. We extracted the lightcurves using regions of the same size as those in the spectral analysis (Sect. 3.3). We used the filtered data between 0.2-10.0 keV and the corresponding GTI (Good Timing Interval) file. This is important as gaps in the data can bias variability tests. We used the *ftool*, *lcstats*[1] (Blackburn, 1995) to perform a Kolmogorov-Smirnov probability of constancy test and the χ^2 probability of constancy test. The results of these tests, along with the size and number of data bins are given in Tables 4 and 5. Several sources in each globular cluster show some evidence for variability. Of these sources, sources 5, 6, 7 and 22 in M 55 show small flares in their lightcurve and sources 11 and 17 appear to show some flickering. Sources 7 and 17's lightcurves can be seen in Figure 5 and those of sources 11 and 22 can be seen in Figure 6. Using a Kolmogorov-Smirnov test, we find that the source lightcurve and the corresponding background lightcurve are statistically different at the 3σ level.

[1] http://heasarc.gsfc.nasa.gov/ftools/

We have also looked at the variability between our observations and previous observations. M 55 was observed with both the *Rosat* cameras: the PSPC (Johnston et al., 1996), and the HRI (Verbunt, 2001). Johnston et al. (1996) observed the cluster between March and April 1993 and found 18 sources in the field of view, where 10 of these fall in the FOV of our observations. The flux limit of this observation is 9.9 $\times 10^{-15}$ergs cm^{-2}s^{-1} (0.5-2.5 keV). Only one source was detected within the core/half-mass radius in both *Rosat* observations, our source 30. This source has varied in flux by a factor three between the two observations, see Table 6. Verbunt (2001) observed the source to have $5\pm1 \times 10^{-4}$ count s^{-1} (0.5-2.5 keV). This gives an unabsorbed flux of 8.1±1.6 $\times 10^{-14}$ergs cm^{-2}s^{-1} (0.5-10.0 keV), consistent with the PSPC observation. Our source 14 was not detected in either of the *Rosat* observations indicating that it was more than 22 times brighter when we observed it in 2001 than during the observations made with the *Rosat* PSPC and should have easily been

Table 4. In the left hand side of the table the best fitting models to spectra from the MOS and *pn* data (with the exception of source 14, which uses only the MOS data as the source fell in a chip gap in the *pn* data and source 6, which uses only the *pn* data as the source is too faint in the MOS), for the sources in M 55. Where no error value is given for the N_H ($\times 10^{21}$cm^{-2}), the N_H was frozen to that of the cluster (0.39×10^{21}cm^{-2} Harris, 1999; Predehl & Schmitt, 1995). The flux given is unabsorbed flux ($\times10^{-13}$ergs cm^{-2}s^{-1}, 0.2-10.0 keV), with errors of the order ±10%. The right hand side of the table contains the results from testing for variability. This includes the number of data bins, the length (in seconds) of each data bin and the probabilities from a Kolmogorov-Smirnov probability of constancy test and the χ^2 probability of constancy test. Source numbers correspond to those given in Table 2 and ^{m} indicates possible cluster members, see Sect. 5.

Src	N_H $\times10^{21}$cm^{-2}	Model	kT (keV)	Photon Index	Abundance	z	χ^2_ν	dof	Flux	bins	time (s)	KS/ χ^2
14	45.82±37.02	PL	-	3.67±2.28	-		0.88	13	22.0	25404	1	4×10^{-8}/
	27.17±22.78	BB	0.64±0.27	-	-		0.88	13				2×10^{-7}
	40.13±29.05	Brems.	1.44±1.18	-	-		0.88	13				
9^m	0.39	PL	-	1.61±0.18	-		0.58	20	0.7	21242	1	9×10^{-3}/
	0.39	BB	0.55±0.06	-	-		1.30	20				5×10^{-5}
	0.39	Brems.	7.99±4.72	-	-		0.63	20				
17^m	0.39	PL	-	2.37±0.19	-		1.48	19	0.80	21231	1	7×10^{-2}/
	0.39	BB	0.36±0.03	-	-		2.79	19				8×10^{-1}
	0.39	Brems.	1.62±0.37	-	-		1.80	19				
	0.39	BB+PL	0.10±0.03	1.91±0.34	-		1.43	17				
7^m	0.39	PL	-	0.69±0.55	-		1.22	6	0.6	21231	1	8×10^{-4}/
	0.39	BB	1.31±0.47	-	-		1.35	6				8×10^{-18}
11^m	0.39	PL	-	2.02±0.19	-		0.61	19	1.1	21222	1	1×10^{-2}/
	0.39	BB	0.37±0.03	-	-		1.48	19				2×10^{-6}
	0.39	Brems.	2.46±0.79	-	-		0.76	19				
	0.39	RS+RS$^@$	0.18,4.45	-			0.52	17				
22^m	0.39	PL	-	1.66±0.33	-		0.80	9	0.8	21067	1	6×10^{-2}/
	0.39	BB	0.40±0.07	-	-		1.64	9				1×10^{-1}
6	34.92±29.00	PL	-	0.93±0.94	-		1.17	15	2.2	21238	1	6×10^{-3}/
	4.00±10.80	BB	2.80±1.32	-	-		1.12	15				2×10^{-3}
5			-	-	-		-	-	0.3	21234	1	5×10^{-3}/
				-	-							5×10^{-2}

PL = power law, BB = blackbody, Brems. = bremsstrahlung, RS = Raymond Smith

$^@$ Errors are ±0.04 and ±1.50 respectively

detected by this instrument if the source had a similar flux in 1993. We do not detect the Johnston et al. (1996) source 5. Our flux limit is 2.6×10^{-15}ergs cm^{-2}s^{-1} (0.5-10.0 keV), twenty times fainter than the source's flux in 1993. We should therefore have detected this source in our observations if it had a similar flux in 2001. This source must also be variable. Other variable sources are source 31, which was a factor 7 times brighter in 1993 and source 11 which was a factor 9 fainter in 1993, see Table 6. Other sources such as sources 9, 17, 22, 10, 49 and 25 have flux values that do not vary between the two observations, within the error values, where the *Rosat* errors are of the order 20-25% of the flux value and the *XMM-Newton* errors bars are 5-25% of the flux value.

NGC 3201 was observed by the *Rosat* PSPC in December 1991 for approximately 2 ks (Johnston et al., 1996). Only four X-ray sources were detected in our field of view, our sources 23, 9, 13 and 20. These sources have not varied between the two observations.

We also searched for periodicities in the barycentre corrected data using a fourier transform to produce a power density spectrum, with the *ftool*, *powspec*. None of the sources showed any strong evidence for a period.

4. The optical counterparts

We constructed a UVW2, (UVW2-B) colour-magnitude diagram with the optical sources found in M 55, see Fig.7. The majority of the optically blue sources in Fig.7 are blue giant stars with UVW2 magnitudes between about 15 and 16 and UVW2-B values between about -0.5 and 1.5. We have identified two blue sources that fall in the positional error circles of the X-ray sources and they can be seen in the colour-magnitude diagram in Fig.7, where the source numbers correspond to those numbers in Table 2. Both of these sources lie within twice the half-mass radius from the centre of the cluster.

Any of the astrometric matches between the *XMM-Newton* X-ray sources and the blue stars may be chance coincidences. We have calculated the number of blue stars per unit area as a function of the radial distance from the centre of the cluster, in the same way as Edmonds et al. (2003a) and Webb et al. (2004c). We have thus been able to calculate the probability of a chance coincidence. We find probabilities of 10% and 2% in the core/half-mass radius and twice the half mass radius respectively. Therefore, it is unlikely that the two blue sources that we have detected in the error circle of the X-ray sources are chance

Table 5. The same as for Table 4 except for the sources in NGC 3201. Source 53 uses only the MOS data. The N_H of the cluster is (1.17×10^{21}cm^{-2} Harris, 1999). Source numbers correspond to those given in Table 3.

Src	N_H $\times10^{21}$cm^{-2}	Model	kT (keV)	Photon Index	Abundance	z	χ^2_ν	dof	Flux	bins	time (s)	KS/ χ^2
26^m	1.17	PL	-	1.90±0.32	-		1.79	14	0.3	28038	1	2×10^{-5}/
	1.17	BB	0.50±0.08	-	-		2.18	14				2×10^{-3}
	1.17	Brems.	3.53±2.48	-	-		1.85	14				
	8.30±7.50	RS	0.97±1.24	-	1.00	0.13±0.25	3.11	12				
23^m	1.29±0.34	PL	-	1.56±0.09	-		1.81	44	2.0	28005	1	3×10^{-1}/
	0.83±0.26	Brems.	13.28±4.33	-	-		1.83	44				1×10^{-1}
22^m	1.17	PL	-	1.54±0.26	-		0.98	9	0.4	28046	1	9×10^{-3}/
	1.17	BB	0.60±0.08	-	-		1.12	9				2×10^{-1}
	1.17	Brems.	8.15±7.42	-	-		0.94	9				
19*	1.17	PL	-	2.02±0.21	-		1.48	17	0.3	27993	1	6×10^{-1}/
	1.17	BB	0.36±0.04	-	-		2.17	17				3×10^{-4}
	0.11±0.77	Brems.	4.94±3.49	-	-		1.57	16				
	0.20±0.61	RS	3.57±1.14	-	1.00	-	1.43	16				
	1.17	BB+PL	0.02±0.00	2.04±0.24	-		1.67	15				
16^{m+}	1.29±0.77	PL	-	1.87±0.24	-		1.24	25	1.0	28530	1	1×10^{-3}/
	1.17	BB	0.40±0.03	-	-		2.36	26				1×10^{-2}
	1.17	Brems.	4.17±1.12	-	-		1.33	26				
	8.52±1.87	RS	1.03±0.13	-	1.00	-	2.90	25				
	1.17	BB+PL	0.25±0.06	1.36±0.46	-		1.22	24				
	1.17	RS+RS	6.79+1.04@		-		1.23	24				
9^m	1.17	PL	-	1.76±0.15	-		0.89	27	1.3	28098	1	2×10^{-5}/
	1.17	BB	0.44±0.04	-	-		1.78	27				2×10^{-2}
	1.17	Brems.	5.33±2.29	-	-		0.93	27				
	9.78±1.91	RS+RS	4.82+0.17[1]		-		0.73	24				
33	1.17	PL	-	1.50±0.11	-		1.31	24	1.1	28050	1	9×10^{-4}/
	1.17	BB	0.44±0.03	-	-		3.79	24				1×10^{-4}
	1.17	Brems.	18.26±14.60	-	-		1.47	24				
	1.17	MEKAL	108.9±45.5	-	2.47±1.27	0.69±0.07	1.37	22				
53	3.16±2.28	PL	-	2.31±0.63	-		0.64	13	2.0	33559	1	1×10^{-7}/
	1.17	BB	0.45±0.05	-	-		0.97	14				2×10^{-1}
	1.79±1.50	Brems.	3.64±2.89	-	-		0.71	13				
	1.67±1.33	RS	4.32±4.22	-	1.0		0.65	13				
13			-	-	-		-	-	6.0	28019	1	4×10^{-5}/
				-	-							1×10^{-3}

PL = power law, BB = blackbody, Brems. = bremsstrahlung, RS = Raymond Smith

@ Errors are ±4.54 and ±0.31 respectively. [1] Errors are ±2.92 and ±0.08 respectively

* Neutron Star Atmosphere (NSA) model, log(T)=6.61±0.04 K, Mass = 1.4 $M_\odot$ (frozen), Radius = 6.96±5.51 km, χ^2_ν = 2.09 (16 d.o.f.)

+ NSA, log(T)=6.83±0.03 K, Mass = 1.4 $M_\odot$ (frozen), Radius = 5.06±0.26 km, χ^2_ν = 1.33 (25 d.o.f.)

+ NSA+PL, log(T)=6.30±0.12 K, Mass = 1.4 $M_\odot$ (frozen), Radius = 10 km (frozen), Γ=1.04±0.63, χ^2_ν = 1.21 (24 d.o.f.)

coincidences, and indeed the optical counterparts to the X-ray sources. We do not find an optical counterpart for many other X-ray sources, but this may be due to the fact that many of the UV sources in the field of view can not be properly resolved.

To find optical counterparts to the X-ray sources in NGC 3201 and to the X-ray sources in M 55 for which we have not been able to find counterparts in our optical data (as they could be binaries which have red (cool) optical counterparts), we have also cross-correlated several catalogues that contain known variable stars in the two globular clusters (Olech et al., 1999; Pych et al., 2001; Mazur et al., 2003; von Braun & Mateo, 2002). None of the variable stars in these catalogues fall within the error circles of our X-ray sources. However, Samus' et al. (1996) find a variable star (their number 51) that is coincident with our source 26 in NGC 3201, the most central source of the cluster. Côté et al. (1994) undertook a search for spectroscopic binaries in NGC 3201 using radial velocity variations. They find sources 215, 216, 248 and 351 respectively (Côté et al., 1994) that fall within the error circles of our X-ray sources 26, 68 and 63 respectively. However, they find no evidence for binarity of these sources.

We also detect several of the optical sources given in the catalogues above in our optical data of M 55, where both the positions and magnitudes are in good agreement with the published data.

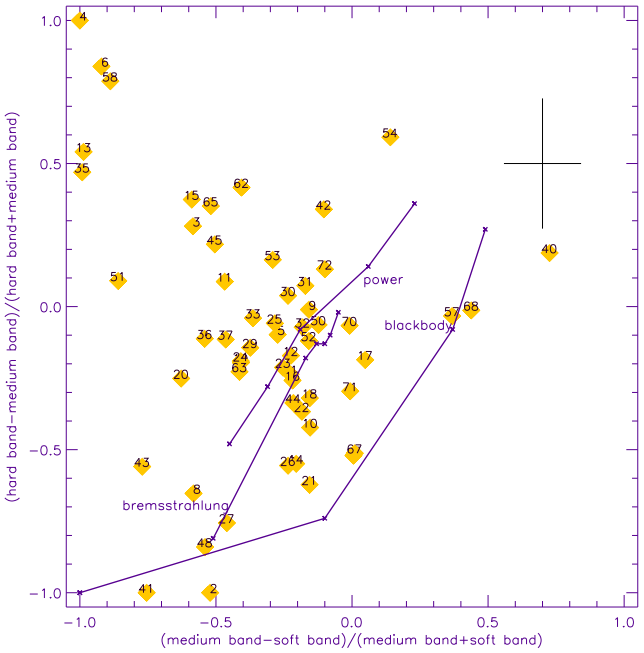

Fig. 4. As Fig. 3, but for NGC 3201. The only difference in the symbols is that on the bremsstrahlung spectrum line, the crosses (from bottom to top) represent temperatures of 1.0, 5.0, 10.0, 20.0 and 50.0 keV.

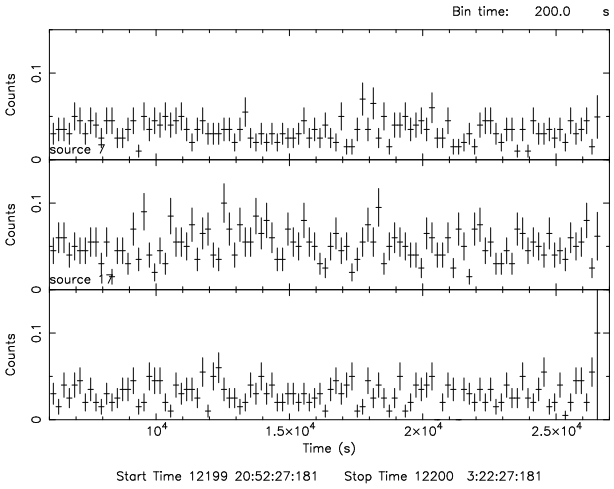

Fig. 5. Lightcurves of two of the sources in M55, top: source 7 and middle: source 17. The lower panel is a typical background lightcurve for these two sources. All of the lightcurves have been plotted on the same scale for ease of comparison and the bin size is 200 seconds, as indicated in the top right hand corner. The first 6000 seconds of this observation were affected by high background and hence are not analysed or plotted.

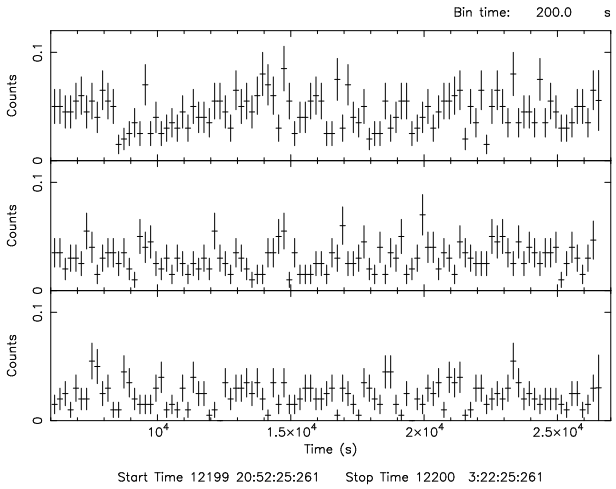

Fig. 6. Lightcurves of two further sources in M55, top: source 11 and middle: source 22. Again the lower panel is a typical background lightcurve for these two sources. All of the lightcurves have been plotted on the same scale for ease of comparison and the bin size is again 200 seconds. As before, the first 6000 seconds of this observation were affected by high background and hence are not analysed or plotted.

Table 6. Sources in M 55 found to be variable between these and the Johnston et al. (1996) observations (data taken in March to April 1993). In the left hand side of the table, the source number is that given in Table 2. The unabsorbed flux (ergs cm^{-2}s^{-1}) is that calculated using the spectrum found through spectral fitting or through the colour analysis (see Fig. 3) in the band 0.5-10.0 keV. In the right hand side of the table, we give the Johnston et al. (1996) count rates in the 0.5-2.5 keV band and their source number (ID). In the final column, we calculate the unabsorbed flux (ergs cm^{-2}s^{-1}) assuming the same spectral fit as used in the left hand of the table. This is again quoted in the 0.5-10.0 keV band.

Source No.	Unabsorbed Flux ($\times 10^{-14}$)	Count rate ($\times 10^{-3}$ cnt s^{-1})	ID	Unabsorbed Flux ($\times 10^{-14}$)
30	3.0±0.6	1.55±0.35	9	8.3 ±2.0
14	22.0±2.0	0.0	-	<0.99
-	<0.26	1.65±0.45	11	-
31	1.0±0.2	3.84±0.55	12	7.0±0.9
11	18.0±0.9	1.54±0.40	8	2.0±0.5

5. Discussion

5.1. Cluster evolution

Mass segregation is well known to exist in the majority of clusters, see Meylan & Heggie (1997) for a review. Certain globular clusters, such as ω Centauri, have been found to be exceptions to the rule. It is thought that the lack of mass segregation in this cluster could be due an unusual dynamical evolution of the cluster, through perhaps the accretion of a stellar system, see Gendre et al. (2003a) and references therein.

The X-ray sources belonging to the globular clusters are thought to be mainly degenerate objects and binary systems. Those sources belonging to M 55 (see Section 3.1) are located in the centre of the cluster, consistent with the idea that the cluster has undergone mass segregation. However, the distribution of X-ray sources in NGC 3201 (see Section 3.2), which appear to be evenly dispersed throughout the cluster, up to

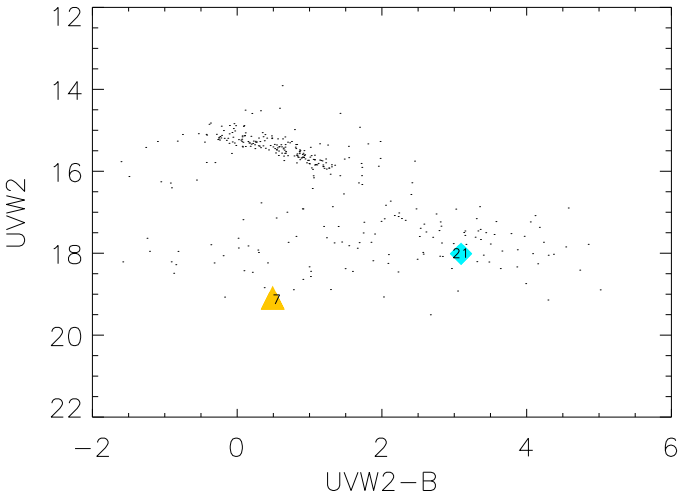

Fig. 7. The UVW2, UVW2-B diagram of the globular cluster M 55. The points show the optical sources and the triangle and diamond show the position of the optical couterparts to the X-ray source with the identification number given on the symbol (as given in Table 2).

five core radii, indicates that the cluster may be slightly disrupted. NGC 3201 is a slightly unusual cluster as its orbit is retrograde with respect to the Galaxy (Gonzalez & Wallerstein, 1998; van den Bergh, 1993). It was originally thought that the cluster may have been captured by our Galaxy, but Gonzalez & Wallerstein (1998) state that since the eccentricity of NGC 3201's orbit is not yet known, it is possible that it is an ordinary member of the halo population. They also remark that NGC 3201's velocity component in the plane of the Milky Way is none the less unique. Côté et al. (1995) also find evidence for possible structure in the velocity field of the stars of the cluster. They state that this could be due to several things including the stripping of stars of the cluster from prolonged interaction with the Galactic tidal field. This can perturb the cluster (e.g. Gnedin & Ostriker, 1997), which could result in the perturbation of the mass segregation. Indeed, Heinke et al. (2003) state that globular clusters undergoing disruption should contain an apparent excess of binaries and binary products, which could explain the apparently large number of X-ray sources belonging to the cluster.

5.2. Cluster members

Here we discuss sources that may be cluster members and their possible nature. The following subsections are summarised in Table 7, where we give all the sources that are possible cluster members, along with their possible nature and luminosity if they are cluster members.

5.2.1. Cataclysmic variables

We find several sources in each cluster which could be cataclysmic variables (CVs). CVs have X-ray spectra that are well fitted by high temperature bremsstrahlung models e.g. (Richman, 1996; Gendre et al., 2003a), with luminosities of up to approximately $1{\times}10^{32}$ erg s^{-1} (0.5-2.5 keV) (Verbunt et al., 1997). They are variable on short (seconds) to long (hours/days) timescales. We expect that such objects should be found towards the centre of the cluster, if the cluster has undergone mass segregation.

In M 55 source 9 has all of the aforementioned characteristics. Verbunt (2001) stated that our faint source 30 (his source X9) could be related to the cluster. It has been noted to be variable, see Section 3.4, being 3 times fainter during our observations than when it was observed by the *Rosat* PSPC in March 1993 *and* by the HRI in September 1997. Kaluzny et al. (2005) observed M 55 over eight observing seasons spanning the period 1997-2004, in U, B, V and I_c. They observed six outbursts of a source that they call CV1 and believe to be a dwarf nova. CV1 has V= 21.88±0.06, B-V= 0.63±0.08, U-B=-0.83±0.09 and V-I= 1.18±0.09 during quiescence and V= 18.98±0.02, B-V= 0.13±0.02, U-B=-0.66±0.03 and V-I= 0.26±0.03 during outburst. Kaluzny et al. (2005) state that the variability of CV1 along with its observed colours indicates that it is a cataclysmic variable of the dwarf nova type. They also state that the available data do not allow them to establish with confidence the cluster membership status of CV1, but that the range of observed luminosities of the variable, 18 <V< 21.8, is consistent with the assumption that it is a bright, non-magnetic dwarf nova belonging to M55. They also indicate that the Rosat source X9 may be the X-ray counterpart and that the X-ray-to-optical luminosity ratio would be higher than average for dwarf novae but consistent with that for SS Cyg, assuming CV1 was in quiescence during *Rosat* observations.

CV1 falls within 3.65″ of our source 30, well within the positional error circle of radius 6.98″ (see Table 2) and is therefore likely to be the optical counterpart to source 30. Looking at the X-ray colour-colour diagram (see Fig. 3), this source is well fitted by a high temperature bremsstrahlung model, indicative of a CV. It appears from our observations that CV1 was not in quiescence during the *Rosat* observations. Kaluzny et al. (2005) state that they observed this source in outburst 23 nights out of the 193 that they observed the cluster, thus 12% of the time. If we assume that this is the average time that the source spends in the outburst state, the chance of observing this source in outburst twice in two observations is only 1.5%. However, large variations in the X-ray flux of cataclysmic variables have been observed during quiescence (e.g. Baskill et al., 2005). If we assume, therefore, that source 30 was in quiescence during our observations, where the lightcurve that we extract appears to be of a fairly constant level, we find that the F_x/F_{opt}= 1.6, where the F_x value is calculated in the 0.5-2.5 keV band as Edmonds et al. (2003b) and Verbunt et al. (1997), using a slightly absorbed, 1 keV thermal bremsstrahlung model and $F_{opt} = 10^{-0.4V-5.43}$. This is still higher than average for a field dwarf nova, but compatible with a field magnetic system, see Figure 18 in Edmonds et al. (2003b). However, Edmonds et al. (2003b) discuss the fact that the cataclysmic variables (and millisecond pulsars) in the globular cluster 47 Tuc have much higher F_x/F_{opt} ratios than field CVs and millisecond pulsars. They find that the cumulative distribution for F_x/F_{opt} of the

47 Tuc CVs follows that of the non-magnetic, low mass transfer rate field CVs rather than that of the magnetic CVs and conclude, after considering the optical magnitudes, that these may be low accretion rate CVs.

Assuming that the CV is in the cluster, we find that its luminosity is 5.8×10^{32} ergs s^{-1}, calculated in the 0.1-100 keV band in the same way as Baskill et al. (2005), who analysed 34 ASCA observations of non-magnetic cataclysmic variables. Such a luminosity is greater than that for their non-magnetic CVs in quiescence, where the most luminous is SS Cyg, which has $L_{0.1-100keV}=1.2\times10^{32}$ ergs s^{-1}. It is therefore unclear what type of CV source 30 may be, but optical spectroscopy of this source will help determine its nature.

In NGC 3201 sources 26 (the most centrally located source, that has been found to be variable, see Sec. 4), 23 and 22 all satisfy the above criteria and are likely to be CVs. The nature of source 16 is unclear. Its X-ray spectrum can be equally well fitted by either a neutron star atmosphere model plus a power law or a blackbody plus a power law model (see Table 5) which could indicate that it is a neutron star system. However, we do not expect to see such an object in this low concentration globular cluster (see Section 5.2.2). Source 16's X-ray spectrum can also be equally well fitted by two Raymond Smith models (see again Table 5) indicative of an active binary (see Section 5.2.3). However, it may also be fitted using a high temperature bremsstrahlung model, indicative of a CV.

5.2.2. Neutrons stars

Both quiescent low mass X-ray binaries with a neutron star primaries (qLMXB^{NS}) and millisecond pulsars (MSPs) are expected in globular clusters (e.g. Gendre et al., 2003b; Grindlay et al., 2001). The qLMXBs^{NS} have luminosities between approximately 10^{32} and 10^{33} erg s^{-1} and are often well fitted by hydrogen atmosphere models. It is thought that these objects are formed primarily through collisions, as opposed to from their primordial binaries, where the number of such binaries is a function of the collision rate of the cluster (Gendre et al., 2003b; Pooley et al., 2003; Heinke et al., 2003). Due to the low central density and thus low collision rate of the two globular clusters studied in this paper, we do not expect to find any such objects. Millisecond pulsars can also have soft spectra, that are well fitted by low temperature blackbodies or hydrogen atmosphere models, where the temperature and radius of the emission are those of the heated polar cap (10^6-10^7 K and ~1 km e.g. Zhang & Cheng, 2003; Zavlin & Pavlov, 1998, and references therein). Millisecond pulsars can also have spectra that are well fitted by hard power laws, where the emission is due to particles accelerated in the magnetosphere or spectra composed of the two different types of emission (e.g. Webb et al., 2004a,b). These objects have lower luminosities than qLMXBs^{NS}, unless there is accretion still taking place in the system.

Sources 7 and 22 in M 55 are well fitted by fairly hard power law spectra (see Table 4). However fitting a blackbody model to these spectra (see again Table 4) we find approximate temperatures and radii (source 7, T=$1.5\pm0.5\times10^7$ K and r=200^{+300}_{-200} m and source 22, T=$4.6\pm0.8\times10^6$ K and r=305^{+143}_{-84} m) that are consistent with those expected from MSPs. Their interstellar absorptions are consistent with those of the cluster and their luminosities are consistent with those expected for millisecond pulsars and thus they could be MSPs. We have also found a possible optical counterpart to source 7, see Fig. 7. This is a very blue source, however it is too bright to be the optical counterpart of the MSP, unless the MSP has a companion. Many millisecond pulsars have companions (e.g. Lundgren et al., 1996), but they can also be cool red stars, rather than the hot blue stars which our optical dataset is designed to detect. However, the companion may be close enough that some accretion onto the compact object continues, in the same way as in the accreting millisecond pulsar SAX J1808.4-3658 (Marshall et al., 1998), which could account for the blue nature of the counterpart. Alternatively, the companion star maybe constantly illuminated by the pulsar, as in PSR 1957+20 (Fruchter et al., 1988), which could also account for the blue nature of the counterpart. From their position in Fig. 3 and location in the cluster, sources 42 and 26 could also be MSPs. Source 17 has a spectrum that is best fitted by a blackbody plus a power law. Such spectra have been found to fit qLMXBs^{NS} see (e.g. Campana & Stella, 2003). The luminosity ($L_{0.5-10.0keV}=3.4\times10^{32}$ erg s^{-1}) is also consistent with such a hypothesis, even though we do not expect any such objects in this globular cluster.

There are several sources in NGC 3201 that have soft X-ray spectra (see Fig. 4). However, if this cluster has not undergone mass segregation, we can not constrain the nature of the objects through their position, thus sources 21, 27, 48 and 67 may all be MSPs. As stated above, the nature of source 16 (in NGC 3201) is unclear. It also has a spectrum that is well fitted by either a blackbody plus a power law or a NSA (Neutron Star Atmosphere) model plus a power law. Again, even though we, statistically speaking, do not expect any such objects in this globular cluster, this object may also be a qLMXB^{NS}.

5.2.3. Active binaries

Dempsey et al. (1993) found, following the analysis of 44 active (RS CVn) binaries observed with *Rosat*, that a two temperature thermal plasma model, with typical temperatures of 2×10^6 K (with a scatter of approximately 1-3×10^6 K) and 1.6×10^7 K (with a scatter of approximately 1-4×10^7 K) gave a good description of the RS CVn X-ray spectra. These binaries have similar luminosities to those of CVs.

We find one source in each cluster which, from the luminosities and X-ray spectra, appear to be RS CVn binaries. Source 11 in M 55 is well fitted by a two temperature Raymond Smith model with temperatures of $2.1\pm0.5\times10^6$ K and $5.2\pm1.7\times10^7$ K, with a luminosity consistent with that expected for such active binaries (see Table 7). Source 9 in NGC 3201 is also well fitted by a two temperature Raymond Smith model with temperatures of $2.0\pm0.9\times10^6$ K and $5.6\pm3.4\times10^7$ K and a similar luminosity to the previous RS CVn candidate. Both of the sources show some evidence for variability in their lightcurves, see Tables 4 and 5, which can also be indicative

of magnetic activity on the stellar surface. Source 16 in this cluster may also be an active binary from the spectral fitting, see Table 5, although we see no evidence for variability in its X-ray lightcurve.

5.2.4. Other potential cluster members

At least one of the core/half-mass radius sources in M 55 is likely to be a member of the cluster, see Section 3.1. Source 30, which appears to be a cataclysmic variable from the X-ray and optical data is likely to be a member. As stated in Section 5.2.2, 42 could be a MSP and therefore related. Source 13 may be related to the cluster, from its position in the cluster and X-ray colours (see Fig. 3), but it is unlikely that sources 12 and 14 are members of the cluster (see Section 5.3).

As stated in Sect. 5.2.1, the most centrally located source in NGC 3201 (source 26) is likely to be related to the cluster. At least one of the core sources are likely to be related to the cluster, see Section 3.2. Source 68, the has X-ray colours compatible with a source in the cluster (see Fig. 4) and therefore *may* also be a CV and related to the cluster.

Table 7. Sources which may be related to M55 (top half of the table) and NGC 3201 (bottom half of the table), along with their possible nature and their approximate luminosity in the 0.5-10 keV band ($\times 10^{32}$ergs s^{-1}) if they belong to the cluster. Each list is ordered with the most likely identification to the least likely identification.

Globular cluster	Source	Possible nature	Luminosity ($\times 10^{32}$)
M 55	30	CV	2.2
	9	CV	2.4
	42	MSP	0.4
	11	RS CVn	4.5
	18	MSP	0.8
	37	MSP	0.3
	17	qLMXB^{NS}	3.4
	7	MSP	2.0
	22	MSP	2.7
NGC 3201	26	CV	0.9
	23	CV	6.2
	22	CV	1.2
	9	RS CVn	4.1
	16	CV/qLMXB^{NS}	3.1
	21	MSP	0.3
	67	MSP	0.2
	27	MSP	1.1

5.3. Non-cluster members

The majority of the sources detected in these observations are background sources. In M 55, source 14 appears to be a background source, from the high interstellar absorption alone, which is much greater than that of the cluster. This is not a defining criteria for a background source, as certain objects that exist in globular clusters can have absorption values higher than that of the cluster i.e. cataclysmic variables. CV spectra can be absorbed due to the high intrinsic absorption of the X-rays from the inner disc and/or white dwarf passing through the edge-on accretion disc e.g. one of the CVs in M 80 (Heinke et al., 2003). The variability of this source and the good fit to the spectrum with a low temperature blackbody could indicate that the source is a low mass X-ray binary that contains a neutron star. However it's luminosity in quiescence is too low for it to be such an object. It therefore seems likely that this object is a background object.

Source 6 in M 55 is also likely to be a background object from its interstellar absorption, spectral fit and position in the cluster. Source 28 has an extremely hard spectrum, in fact the hardest of the cluster. It is likely that this source is not actually related to the cluster, but is an Active Galactic Nucleus (AGN). The fact that we find no optical counterpart to this source in our optical data could support this theory, where the optical flux would be redshifted to very red wavelengths. Other sources that are found in the top right hand corner of Fig. 3, that are found towards the exterior of cluster, such sources 27 and 40 are also likely to be background objects.

Kaluzny et al. (2005) have detected a blue source in their observations (described in Section 5.2.1), which they call M55-B1, which has V= 20.40 and U-B=-0.65. This source falls within 2″ of our source 39, well within the error circle of radius 8″. M55-B1 is therefore likely to be the optical counterpart to source 39. From its colours and low-amplitude variability, Kaluzny et al. (2005) propose that this source is a quasar. Source 39 does not appear in the X-ray colour-colour diagram of M 55 (Figure 3). Extracting the spectra, we find that the source is very absorbed and has insufficient counts in the softest band to appear on the diagram. We find that the interstellar absorption is approximately 1×10^{23} cm^{-2}, which could indicate an extragalactic origin for this object.

In NGC 3201, the spectra of sources 19 and 33 are best fitted by a Raymond Smith and a MEKAL model respectively, both indicative of emission from a hot diffuse system, such as a galaxy. They therefore could be extragalactic sources. Sources 4 and 6 are located far from the cluster centre and have spectra consistent with that of an AGN. Source 58 in the half-mass radius, could belong to the cluster (see Section 3.2), however from the X-ray colours, which indicate an absorbed extragalactic source, it is unlikely. Other sources with similar colours such as 6, 13 and 54 may also be background sources.

6. Conclusions

Using *XMM-Newton* X-ray observations of the globular M 55 we detect 47 X-ray sources in the direction of the cluster, any of which belonging to the cluster must have low luminosities. Using the logN-logS diagram derived from Lockman Hole observations to determine the background population, we find that very few of the sources (1.5±1.0) in the FOV of this cluster are likely to belong to the cluster. These sources are found in the central region of the cluster, which implies that this cluster has undergone at least some mass segregation. Through X-ray and

optical colours, spectral and timing analysis (where possible) and comparing these observations to previous X-ray observations, we find two sources that could be cataclysmic variables, one that could be an active binary, several that may be MSPs and possible evidence for a qLMXB^{NS}. The majority of the other sources are background sources such as AGN.

We find 62 X-ray sources in the *XMM-Newton* FOV of NGC 3201, where as many as 15 sources could belong to the cluster. These sources, in contrast to those found in M 55 and in many other Galactic globular clusters are not centrally located, but distributed throughout much of the cluster, which could indicate a perturbation of the cluster. Using X-ray observations only, we find three/four sources that could be CVs, one that could be an active binary, several that may be MSPs and again possible evidence for a qLMXB^{NS}, although again we do not expect any such objects, statistically speaking, in either of the clusters, due to their low central concentrations. Again, the majority of the other sources are background sources.

Acknowledgements. This article was based on observations obtained with XMM-Newton, an ESA science mission with instruments and contributions directly funded by ESA Member States and NASA. The authors NAW and DB also acknowledge the CNES for its support in this research.

References

Baskill, D.S., Wheatley, P.J., Osborne, J.P. 2005, MNRAS, 357, 626
Blackburn, J. K. 1995, in ASP Conf. Ser., Vol. 77, Astronomical Data Analysis Software and Systems IV, ed. R. A. Shaw, H. E. Payne, and J. J. E. Hayes (San Francisco: ASP), 367
Campana, S., & Stella, L. 2003, ApJ, 597, 474
Chernoff, D.F., Kochanek, C.S., & Shapiro, S.L. 1986, ApJ, 309, 183
Cool A.M., Grindlay, J.E., Bailyn, C.D., Callanan, P.J., & Hertz, P. 1995, ApJ, 438, 719
Cool A.M., Haggard D., & Carlin J.L. 2002, ASP conf. series, 265, 277
Côté, P., Welch, D. L., Fischer, P., Da Costa, G. S., Tamblyn, P., Seitzer, P., & Irwin, M.J. 1994, ApJS, 90, 83
Côté, P., Welch, D. L., Fischer, P., Da Costa, & Gebhardt, K. 1995, ApJ, 454, 788
Covey, K.R., Wallerstein, G., Gonzalez, G., Vanture, A.D., & Suntzeff, N.B. 2003, PASP, 115, 819
Dempsey, R.C., Linsky, J.L., Schmitt, J.H.M.M., & Fleming, T.A. 1993, ApJ, 413, 333
Djorgovski S., 1993, ASP conf. series, 50, 373
Edmonds P.D., Gilliland R.L., Heinke C.O., & Grindlay , J.E. 2003a, ApJ, 596, 1177
Edmonds P.D., Gilliland R.L., Heinke C.O., & Grindlay , J.E. 2003b, ApJ, 596, 1197
Fruchter, A.S., Gunn, J.E., Lauer, T.R., & Dressler, A. 1988, Nature, 334, 686
Geffert, M., Aurière, M., & Koch-Miramond, L., 1997, A&A, 327, 137
Gendre, B., Barret, D., & Webb, N.A. 2003a, A&A, 400, 521
Gendre B., Barret D., & Webb N.A. 2003b, A&A, 403, L11
Gnedin, O.Y., & Ostriker, J.P. 1997, ApJ, 474, 223
Gonzalez, G., & Wallerstein, G. 1998, AJ, 116, 765
Grindlay, J.E., Heinke, C., Edmonds, P.D., & Murray, S. S. 2001, Sci., 292, 2290
Harris W. E., 1999, Ap&SS, 267, 95
Hasinger G., Altieri B., Arnaud M., et al., 2001, A&A, 365, L45
Heinke, C.O., Grindlay, J.E., Edmonds, P.D., Lloyd, D.A., & Murray, S.S. 2003, ApJ, 598, 516
Hénon, M. 1961, AnAp, 24, 369
Hertz P., & Grindlay J. 1983, ApJ, 275, 105
Hertz P., & Wood, K.S. 1985, ApJ, 290, 171
Hut, P., McMillan, S., Goodman, J., et al. 1992, PASP, 104, 981
Johnston H.M., Verbunt F., & Hasinger G. 1994, A&A, 289, 736
Johnston H.M., & Verbunt F. 1996, A&A, 312, 80
Johnston, H.M., Verbunt, F., & Hasinger, G. 1996, A&A, 309, 116
Kaluzny, J., Pietrukowicz, P., Thompson, I. B., Krzeminski, W., Schwarzenberg-Czerny, A., Pych, W., & Stachowski, G. 2005, MNRAS, 359, 677
Kirsch, M., and the EPIC Consortium, 2002, XMM-SOC-CAL-TN-0018
Layden, A.C., & Sarajedini, A. 2003, AJ, 125, 208
Lundgren, S.C., Cordes, J.M., Foster, R.S., Wolszczan, A., & Camilo, F. 1996, ApJ, 458, 33
Mandushev, G.I., Fahlman, G.G., & Richer, H.B. 1997, AJ, 114, 1060
Marshall, F.E., Wijnands, R., & van der Klis, M. 1998, IAUC, 6876
Mason K. O., Breeveld, A., Much, R. et al., 2001, A&A, 365, L36
Mazur, B., Krzeminski, W., & Thompson, I. B. 2003, MNRAS, 340, 1205
Meylan, G., & Heggie, D.C. 1997, A&A Rev., 8, 1
Pych, W., Kaluzny, J., Krzeminski, W., Shwarzenberg-Czerny, A., & Thompson, I. B. 2001, A&A, 367, 148
Piersimoni, A.M., Bono, G., & Ripepi, V. 2002, AJ, 124, 1528
Piotto, G., & Zoccali, M. 1999, A&A, 345, 485
Pooley, D., Lewin, W.H.G., Anderson, S.F., et al. 2003, ApJ, 591, 131
Predehl, P. & Schmitt, J. H. M. M. 1995, A&A, 293, 889
Pych, W., Kaluzny, J., Krzeminski, W., Schwarzenberg-Czerny, A., & Thompson, I. B. 2001, A&A, 367, 148
Pye, J.P., & McHardy, I.M. 1983, MNRAS, 205, 875
Richman, H.R. 1996, ApJ, 462, 404
Rutledge, R.E., Bildsten, L., Brown, E.F., Pavlov, G.G., & Zavlin, V. E. 2002, ApJ, 578, 405
Samus', N. N., Kravtsov, V. V., Pavlov, M. V., Strel'Nikov, V. V., Shokin, Yu. A., Alcaino, G., Liller, W., & Alvarado, F. 1996, PAZh, 22, 269
Turner, M.J.L., Abbey, A., Arnaud, M. et al. 2001, A&A, 365, L27
Verbunt, F., Bunk, W.H., Ritter, H., & Pfeffermann, E. 1997, A&A, 327, 602
Verbunt, F. 2001, A&A, 368, 137

Verbunt F., & Lewin, W.H.G., 2004, Chapter 8 in ”Compact Stellar X-ray Sources”, eds. W.H.G. Lewin and M. van der Klis, Cambridge University Press
van den Bergh, S. 1993, ApJ, 411, 178
von Braun, K., & Mateo, M. 2002, AJ, 123, 279
Webb, N.A., Gendre, B., & Barret, D. 2001, A&A, 381, 481
Webb, N.A., Olive, J.F., & Barret, D. 2004a, A&A, 417, 181
Webb, N.A., Olive, J.F., Barret, D., Kramer, M., Cognard, I., & Löhmer, O. 2004b, A&A, 419, 269
Webb, N.A., Serre, D., Gendre, B., Barret, D., Lasota, & J.-P., Rizzi, L. 2004c, A&A, 424, 133
Zaggia,S.R., Piotto, G., & Capaccioli, M. 1997, A&A, 327
Zavlin, V.E., & Pavlov, G.G. 1998, A&A, 329, 583
Zhang, L., & Cheng, K.S. 2003, A&A, 398, 639